

MCNP performance on neutronic calculation of VERA benchmark cases

Zuhair* , Wahid Luthfi , Entin Hartini , Sriyono ,
Suwoto , Deswandri 

Research Center for Nuclear Reactor Technology ORTN-BRIN BJ Habibie Science and Technology Area, Serpong, Tangerang Selatan, Indonesia.

*Corresponding author: zuhair@brin.go.id

Original Research

Abstract:

Received:
21 February 2024
Revised:
3 March 2024
Accepted:
4 April 2024
Published online:
25 May 2024

© The Author(s) 2024

VERA benchmark cases have been introduced by ORNL and detailed guidelines have been provided including the burnup chain data for a depletion analysis. The purpose of this paper was to analyze the performance of MCNP Monte Carlo code using VERA benchmark cases. Research on the VERA benchmark cases become important because its results will be useful for designing SMRs planned in the country. The VERA 2B and VERA 2P were selected as a representation for a typical fuel assembly of LWR configurations. The k_{inf} MCNP calculations show a good agreement with the MCS and STREAM predictions at the Beginning of Cycle (BOC), Middle (MOC), and End (EOC). The k_{inf} value at BOC calculated using MCNP for VERA 2B case shows a good agreement compared to KENO, Serpent, and OpenMC with a difference of less than 60 pcm while for VERA 2P case with a difference of less than 90 pcm. Doppler Temperature of reactivity Coefficient (DTC) and Moderator Temperature (MTC) results were negative and both became more negative as fuel burnup increased. The β_{eff} values of both cases were close to 670 pcm during BOC since both cases use ^{235}U fissile nuclear material. The ^{239}Pu production in VERA 2B was higher than 2P since higher ^{238}U in 2B and 24 pins of mixed lower enrichment and gadolinium in 2P lowers its heavy metal loading followed by the neutron spectrum shifting. It can be concluded that these results can be used in the development of computational performance for overall core analysis to strengthen the basic design of the SMR to be built in Indonesia.

Keywords: Criticality; VERA benchmark cases; MCNP; ENDF/B-VII.1

1. Introduction

Indonesia is the largest archipelagic country in the world with most of its territory consisting of small islands. The need for electrical energy on these small islands was only a few hundred megawatts of electricity (MWe) and the power demand in these remote areas [1] can be fulfilled by Small Modular Reactors (SMR). SMR has the advantage that it can be built in remote areas that are difficult to reach and do not have the infrastructure to transport fuel. Another advantage of SMR technology is a simpler modular design, developed with passive safety systems, long life cycles, and resistance to proliferation [2]. SMRs become a trend in advanced nuclear reactor technology, especially to reduce the initial capital cost investment

typically required by large-scale nuclear power plants [3]. Advanced SMRs can provide affordable nuclear power options while ensuring safe and clean energy. Furthermore, the advanced SMR technology offers not only a simpler modular design in nuclear power generation applications but also safer while being cheaper and easier to manufacture relative to a typical large-scale reactor by the economy of scale [4, 5]. Water-cooled SMR represents a mature technology considering that most of the nuclear power plants operating today are water-cooled reactors. Therefore, around twenty-five designs of water-cooled SMR use either light water or heavy water technologies for large to small remote grid applications, also for district heating [6]. The SMR design was proposed since its simpler and safer

safety concept relies on a passive system with safety characteristics inherent in the reactor [7]. In recent years, research to design SMRs was promoted through the Virtual Environment for Reactor Applications (VERA) benchmark cases [8]. VERA benchmark cases have been introduced by Oak Ridge National Laboratory (ORNL) and detailed guidelines have been provided including the burnup chain data for a depletion analysis. The VERA benchmark cases consist of 9 cases of single pin (SP) and 16 cases of fuel assembly (FA) with various fuel temperatures, ^{235}U enrichments, control rods, and burnable poisons. These benchmark cases can be used to validate the neutron transport code's capability in calculating criticality and neutronic parameters.

Various studies on the modeling and simulation of VERA benchmark cases have been performed since the benchmark results were provided by Kim in 2018 [9]. Park consistently compared depletion calculations between four neutronic analysis codes with the VERA depletion problems [10]. Yu verified the OpenMC capability using the VERA depletion benchmark for all 26 cases including 10 pin-cell cases and 16 fuel assembly cases, and also carried out comparisons with published KENO results [11]. In Park's study, McCARD burnup analyses for the VERA depletion benchmarks were performed to examine its newly implemented depletion analysis modules [12]. Albugami presented results to VERA benchmark problems utilizing the OpenMC code and showed a code-to-code comparison with CASL VERA data [13]. Collins simulated the BEAVRS benchmark using VERA [14] while Nguyen presented a benchmark solution to the VERA problem using MCS codes with a study consisting of code-to-code comparisons with KENO-VI and Serpent 2 [15]. Mai analyzed several VERA benchmark problems with the deterministic transport code STREAM for 2D and 3D calculations [16]. All the codes performed their depletion capability to simulate the VERA benchmark with good results. In this study, it was expected that the MCNP6 would show its ability to accurately predict

the criticality and nuclide composition of VERA benchmark fuel.

The purpose of this paper was to develop fuel assembly from VERA benchmark cases using MCNP Monte Carlo code and providing the Doppler temperature coefficient (DTC) of reactivity, the moderator coefficient of reactivity (MTC) and effective delayed neutron fraction (β_{eff}) on each case. The VERA 2B and VERA 2P were selected as a representation for a typical fuel assembly of light water reactor (LWR) configurations. These benchmark cases were 2D fuel lattices without and with gadolinium. The MCNP code was chosen due to its flexible modeling capability and neutron transport solved using the Monte Carlo method with continuous energy nuclear data library [17]. MCNP tracks the neutron history started from the initiated source particle position and fission neutron while ENDF/B-VII.1 nuclear data library was used in this study, also the CINDER module was used to calculate fuel burnup for up to 60 MWd/kg [18, 19]. The neutronic parameters resulting from both benchmark cases can then be compared with VERA benchmark results and the various studies using other neutronic codes.

2. Materials and methods

2.1 VERA benchmark cases

VERA benchmark cases have been developed to test the performance of neutronic code, evaluate computational model, and validate their result by performing a code-to-code comparison. Table 1 presents the geometrical and material data for VERA 2B and 2P benchmark cases consisting of a fuel assembly on 17×17 fuel pins configuration, made up of 264 fuel rods, 24 guide tubes, and one instrumentation tube.

2.2 Calculation model

In this work, a series of calculations have been carried out from VERA benchmark cases using MCNP code with ENDF/B-VII.1 library to evaluate users' capability to develop those cases. MCNP was a well-established Monte

Table 1. Geometry and material data for VERA 2B and 2P benchmark cases.

Core	
Pressure (bar)	155.13
Power density (W/gU)	40.00
Fuel assembly power (MW/cm)	0.050324728
Assembly pitch (cm)	21.5000
Pin pitch (cm)	1.2600
Fuel	
Pellet radius (cm)	0.4096
Material	UO ₂ (3.1% ^{235}U)
Density (g/cm ³)	10.2570
Gadolinium rod	
Pellet radius (cm)	0.4096
Material	UO ₂ (1.8% ^{235}U) + 5% Gd ₂ O ₃
Density (g/cm ³)	10.1110
Cladding	
Inner radius (cm)	0.4180
Outer radius (cm)	0.4750
Material	Zircaloy-4
Density (g/cm ³)	6.5600

Carlo transport code that can model 3-dimensional complex geometry including the reactor core and all its components to analyze interactions between radiation and matter using its continuous neutron energy spectra. MCNP has successfully demonstrated its capability in simulating the neutronic behavior of various reactors [20–37].

The VERA 2B fuel assembly consists of 264 UO_2 fuel pins with 3.1% ^{235}U enrichment while the VERA 2P fuel assembly uses 240 fuel pins of this type with additional 24 fuel pins of mixed $\text{UO}_2+\text{Gd}_2\text{O}_3$, with 1.8% ^{235}U enrichment and 5%wt. of Gd. Gadolinium (Gd_2O_3) was used as a burnable poison since it was a neutron absorber that burned (depleted) during reactor operation. From these models, it was known that the VERA 2P case would have lower fissile material content and lower heavy metal loading due to these 24 mixed fuel pins.

The VERA benchmark cases consist of a fuel pin which was a fuel rod surrounded by a helium gap inside a Zircaloy-4 clad with the dimensions mentioned in Table 1. Water as a coolant and moderator with a boron concentration of 1300 ppm surrounds the fuel pin, making up a fuel lattice with a pitch of 1.2600 cm. The moderator, cladding, and fuel temperatures were set to 600 K and 900 K for the VERA 2P fuel assembly while for the VERA 2B was set to 600 K. The guide tube and instrumentation tube as part of the structure were designed to guide the movement of the control rod and provide space for detectors, in-core instrumentation, and other measurement tools for monitoring the reactor core. Both tubes were modeled by modeling a tube with the size mentioned in Table 1 and the same lattice pitch as the fuel pin lattice pitch. The MCNP model for the fuel pin, guide tube, and instrumentation tube is shown in Figure 1 while the atomic number density for each material is presented in Table 2.

The VERA 2B and 2P benchmark cases were fuel assem-

blies arranged in a square lattice of 17×17 configuration with a fuel assembly size of 21.50 cm. These fuel assemblies were modeled by arranging 264 standard fuel pins for case 2B while for case 2P, the 240 standard fuel pins and 24 fuel with gadolinia pins were used, with both cases using 24 guide tubes and 1 instrumentation tube. The MCNP models for both cases are seen in Figure 2.

The total neutron histories employed for k_{inf} calculations was 125 million neutrons using 500,000 neutrons per cycle with 300 total cycles (50 inactive), giving a statistical uncertainty of around 6 pcm. The initial fission neutron source was located at the center of the fuel pin, making a 264-point source at the middle of each fuel pin. Thermal scattering data $S(\alpha, \beta)$ for light water was applied while reflective boundary conditions were used on all six surfaces of the fuel assembly. The burnup calculation was performed with a thermal power density of 40.0 W/gU, analog to 18.41 MW for the 365.76 cm height of the modeled fuel assembly. The burnup calculation starts from 0.0, 0.01, 0.25, 0.50, 0.75 to 1.0 MWd/kgU, followed by the interval of 1 MWd/kgU for 1 – 20 MWd/kgU and the interval of 2.5 MWd/kgU for 20 – 60 MWd/kgU. The Beginning of Cycle (BOC) was defined as 0 MWd/kgU while the Middle of Cycle (MOC) was 30 MWd/kgU and the End of Cycle (EOC) for 60 MWd/kgU. The MCNP simulation was carried out using a workstation with specification Intel(R) Core(TM) i7-X5960CPU, 3.0GHz-6core, RAM 32GB, with execution time of ~ 2460 minutes for each case.

The calculated multiplication factors will be compared to benchmark results (McCARD) [9] and previous studies that use OpenMC [11], MCS [15, 38], and STREAM [19, 39] codes. OpenMC was an open-source Monte Carlo transport code, while MCS was developed by the Ulsan National Institute of Science and Technology (UNIST) which both could solve 3-D continuous-energy neutron physics code

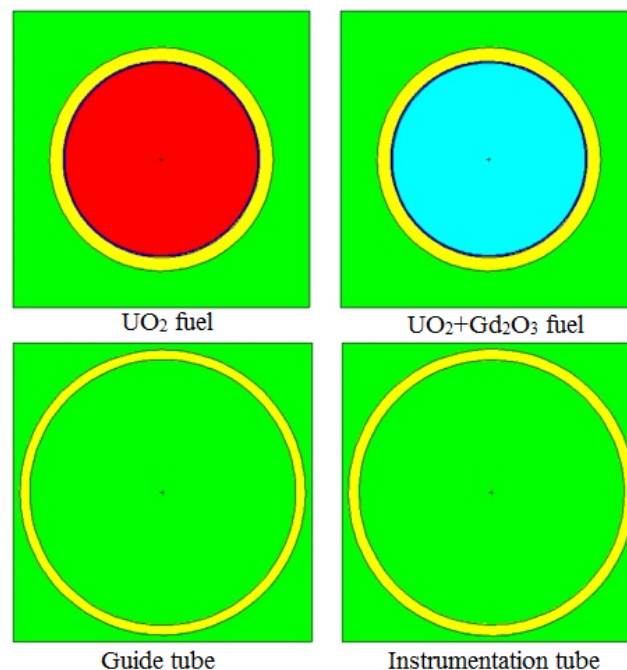


Figure 1. MCNP model for fuel cell, guide tube and instrumentation tube.

for particle transport based on the Monte Carlo method. STREAM was a deterministic neutron transport analysis code developed to use the method of characteristics to solve the multi-group neutron transport equation for 2D and 3D core analysis, also developed by UNIST.

The Doppler temperature coefficient (DTC) of reactivity, the moderator coefficient of reactivity (MTC), and the effective delayed neutron fraction (β_{eff}) were also calculated for each case. The DTC also known as fuel temperature reactivity coefficient came from the Doppler broadening in the resonance region of neutron interaction cross-sections of the fertile material (^{232}Th , ^{238}U , ^{240}Pu). While MTC was correlated with changes in moderator temperature and density both MTC and DTC were considered dominant temperature reactivity coefficients which became part of the inherent safety parameters in nuclear reactors. The DTC and MTC were calculated by the following equation:

$$\text{DTC} = \frac{k_2 - k_1}{k_2 \times k_1} \frac{1}{\Delta T} \quad (1)$$

$$\text{MTC} = \frac{k_3 - k_1}{k_3 \times k_1} \frac{1}{\Delta T} \quad (2)$$

with k_1 was the multiplication factor with moderator and fuel temperature at 600 K for VERA 2B and 900 K for

VERA 2P, while k_2 was calculated with moderator temperature at 600 K while fuel was at 1200 K. k_3 was calculated with moderator temperature of 565 K for 600 K fuel temperature for VERA 2B and 900 K fuel temperature for VERA 2P. From this equation, negative values in both DTC and MTC correlate with a decrease in reactivity when its corresponding physical temperature increases.

On another hand, the effective delayed neutron fraction (β_{eff}) was calculated using the Iterated Fission Probability (IFP) that has been implemented on MCNP.

3. Results and discussion

The infinite multiplication factor (k_{inf}) or criticality result of VERA 2B and 2P benchmark cases is seen in Table 4 while Table 4 shows its comparison to other codes. In comparison to the MCS and STREAM code, MCNP shows a good agreement at the BOC with a difference of less than 100 pcm. The Monte Carlo method was implemented on MCNP and MCS gives a different response on depletion calculation so that the k_{inf} at MOC and EOC were differentiated on both codes within the range of 200 – 700 pcm. The difference between MCNP to STREAM shows a great discrepancy for case 2P of fuel assembly with burnable absorber during the BOC that can be rooted in the difference in multigroup cross sections generated for STREAM and its

Table 2. Atomic number density for each material.

Fuel UO ₂ (3.1% ²³⁵ U enrichment)					
²³⁴ U	6.11864E-06	²³⁶ U	3.29861E-06	¹⁶ O	4.57642E-02
²³⁵ U	7.18132E-04	²³⁸ U	2.21546E-02		
Fuel UO ₂ + Gd ₂ O ₃ (1.8% ²³⁵ U enrichment, 5% Gd concentration)					
²³⁴ U	3.18096E-06	¹⁵² Gd	3.35960E-06	¹⁵⁷ Gd	2.62884E-04
²³⁵ U	3.90500E-04	¹⁵⁴ Gd	3.66190E-05	¹⁵⁸ Gd	4.17255E-04
²³⁶ U	1.79300E-06	¹⁵⁵ Gd	2.48606E-04	¹⁶⁰ Gd	3.67198E-04
²³⁸ U	2.10299E-02	¹⁵⁶ Gd	3.43849E-04	¹⁶ O	4.53705E-02
Helium					
⁴ He	2.68714E-05				
Cladding					
⁹⁰ Zr	2.18865E-02	¹¹⁸ Sn	1.16872E-04	⁵² Cr	6.36606E-05
⁹¹ Zr	4.77292E-03	¹¹⁹ Sn	4.14504E-05	⁵³ Cr	7.21860E-06
⁹² Zr	7.29551E-03	¹²⁰ Sn	1.57212E-04	⁵⁴ Cr	1.79686E-06
⁹⁴ Zr	7.39335E-03	¹²² Sn	2.23417E-05	¹⁷⁴ Hf	3.54138E-09
⁹⁶ Zr	1.19110E-03	¹²⁴ Sn	2.79392E-05	¹⁷⁶ Hf	1.16423E-07
¹¹² Sn	4.68066E-06	⁵⁴ Fe	8.68307E-06	¹⁷⁷ Hf	4.11686E-07
¹¹⁴ Sn	3.18478E-06	⁵⁶ Fe	1.36306E-04	¹⁷⁸ Hf	6.03806E-07
¹¹⁵ Sn	1.64064E-06	⁵⁷ Fe	3.14789E-06	¹⁷⁹ Hf	3.01460E-07
¹¹⁶ Sn	7.01616E-05	⁵⁸ Fe	4.18926E-07	¹⁸⁰ Hf	7.76449E-07
¹¹⁷ Sn	3.70592E-05	⁵⁰ Cr	3.30121E-06		
Moderator (1300 ppm boron, 600 K)					
¹⁶ O	2.33753E-02	¹⁰ B	1.00874E-05		
¹ H	4.67505E-02	¹¹ B	4.06030E-05		

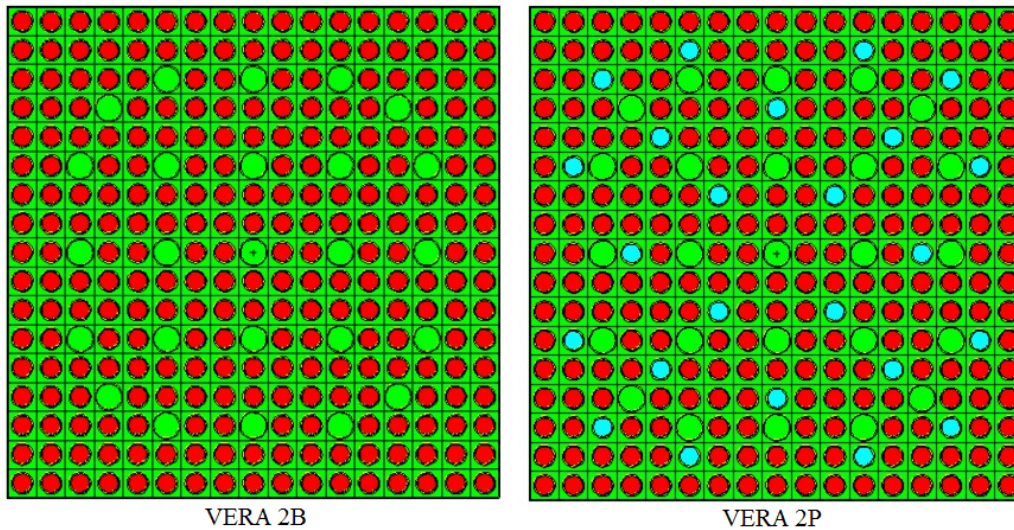


Figure 2. MCNP model for VERA benchmark cases.

treatment for burnable absorber modeled within STREAM. By comparing the calculated results with benchmark data by McCARD, it was found that the results show a good agreement at the BOC, but at MOC-EOC the deviations from the McCARD values were observed to be within the range of 175 – 1500 pcm. This high deviation to benchmark data might come from the difference in nuclear data being used for burnup calculation (depletion chain and nuclear energy-branching ratio) which was ENDF/B-VII.0 for McCARD while our MCNP used ENDF/B-VII.1. Previous studies also showed that the differences between the ENDF/B-VII.0 and ENDF/B-VII.1 were around 30 pcm on fresh pin cell problem [15]. In comparison to other codes, k_{inf} value at BOC calculated using MCNP for VERA 2B case shows a good agreement compared to KENO, Serpent,

and OpenMC with a difference of less than 60 pcm while for VERA 2P case with a difference of less than 90 pcm. Figure 3 illustrates the changes in k_{inf} during fuel burnup for both VERA 2B and 2P benchmark cases that show the burnable poison acting on case 2P to reduce k_{inf} at the beginning of cycle. The sudden k_{inf} drop in both cases at the BOC correlates to the production of ^{135}Xe and ^{149}Sm fission products that absorb neutrons during reactor operation with their equilibrium concentration. The k_{inf} of VERA 2P assembly peaked at ~ 1.02 around 11 MWd/kg when gadolinium (^{155}Gd and ^{157}Gd) was fully depleted, and the decreasing of k_{inf} followed similar trends to the 2B case. Table 5 summarizes the Doppler temperature coefficient (DTC) of reactivity, the moderator coefficient of reactivity (MTC), and the effective delayed neutron fraction (β_{eff})

Table 3. Comparison of calculated k_{inf} by MCNP with MCS [38]; STREAM [39], and McCARD [9].

VERA cases	Burnup condition	MCS	Stream	McCARD	MCNP	Difference* (pcm)		
						with MCS	with Stream	with McCARD
VERA 2B	BOC	1.18291 ± 0.00004	1.18204	1.182710	1.18208 ± 0.00006	-83	+4.0	-6.3
	MOC	0.90010 ± 0.00003	0.90087	0.895640	0.89740 ± 0.00006	-270	-347	+176
	EOC	0.77322 ± 0.00003	0.77438	0.761262	0.77029 ± 0.00006	-293	-409	+902.8
VERA 2P	BOC	0.92677 ± 0.00003	0.92734	0.919643	0.92067 ± 0.00006	-610	-667	+102.7
	MOC	0.87890 ± 0.00003	0.87944	0.885197	0.88344 ± 0.00006	454	+400	-175.7
	EOC	0.74304 ± 0.00003	0.74447	0.760579	0.74568 ± 0.00006	264	+121	-1489.9

*Relative difference = (MCNP-MCS; Stream; McCard) × 100000 pcm.

Table 4. Comparison of calculated k_{inf} by MCNP (ENDF VII.1) with KENO, Serpent and OpenMC (ENDF VII.0) [11].

VERA cases	Burnup condition	KENO	Serpent	OpenMC	MCNP	Difference* (pcm)		
						with KENO	with Serpent	with OpenMC
VERA 2B	BOC	1.18240 ± 0.00012	1.18156 ± 0.00013	1.18217 ± 0.00016	1.18208 ± 0.00006	-32	+52	-9
VERA 2P	BOC	0.91993 ± 0.00016	0.92017 ± 0.00017	0.91983 ± 0.00012	0.92067 ± 0.00006	+74	+50	+84

*Relative difference = (MCNP-KENO; Serpent; OpenMC) × 100000 pcm.

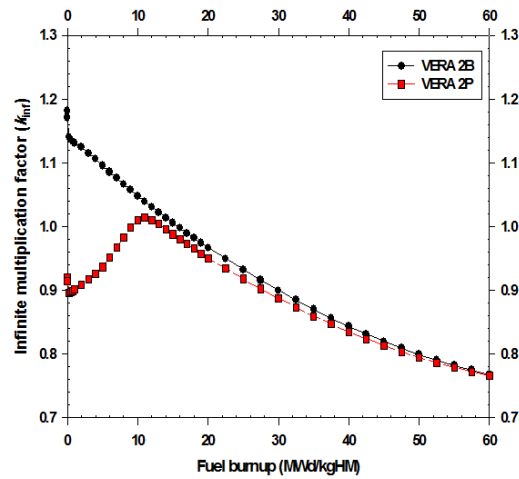


Figure 3. K_{inf} of VERA benchmark cases

in each case. Table 5 shows that the DTC and MTC were all negative, which is below $-4 \times 10^{-5} \Delta k/k \text{ K}^{-1}$ for the VERA 2B case and below $-7 \times 10^{-6} \Delta k/k \text{ K}^{-1}$ for the 2P case. Both became more negative as the fuel burned, ensuring the safety of the reactor from the beginning of reactor operation through the end. Table 5 also confirms that the VERA 2B assembly without Gd_2O_3 content shows a more negative DTC and MTC compared to the VERA 2P assembly containing Gd_2O_3 fuel rods. Since these lower DTC and MTC of the 2P case happened during subcritical conditions at the BOC, the 2P fuel assembly was already reducing core overall reactivity during this burnup step. The effective delayed neutron fraction (β_{eff}) reflects the fraction of delayed neutrons relative to the total neutron population in the reactor, and it was related to the controllability of the reactor. Table 5 shows that the β_{eff} values of VERA 2B and VERA 2P were within the range of 670 – 685 pcm since both cases use ^{235}U fissile nuclear material which has similar fractions of delayed neutrons and delayed neutron precursors. The decrease in β_{eff} value during fuel burnup comes from other fissile materials being produced from the transmutation of ^{238}U , i.e. ^{239}Pu and ^{241}Pu in combination with the remaining ^{235}U within the fuel assembly. The depletion of heavy metals in the VERA benchmark cases was interesting to evaluate since the use of uranium could produce plutonium isotopes through a transmutation

process that becomes the main contribution to fuel proliferation analysis. Since uranium and plutonium isotopes were essential for reactor operation by sustaining the nuclear chain reaction, Figure 4 and Figure 5 show both isotopic elements in each case. As previously mentioned in methodologies, the ^{235}U concentration of VERA 2B fuel assembly at BOC was higher than VERA 2P assembly as could be seen in Figure 4, but towards the EOC their concentrations were almost the same, ~ 1000 gr, which came from the use of 24 mixed uranium (lower enrichment) and gadolinium fuel pins. The use of Gd_2O_3 absorbs neutrons but the depletion gradients of ^{235}U and ^{238}U were not fully affected since the number of fissions should be maintained to achieve the same amount of power, so the neutron flux will be increased to compensate for absorbed neutrons by gadolinia at the beginning of cycle, and these neutron flux not only induce fission but also transmutation on fuel material. Figure 5 illustrates five plutonium isotopes, i.e. ^{238}Pu , which comes from the beta decay of ^{238}Np while ^{238}Np comes from irradiated ^{237}Np , and ^{237}Np comes from irradiated ^{236}U . ^{238}Pu can be used for long-life nuclear batteries, as well as providing a long-lived heat source to power NASA space missions. The ^{238}Pu and ^{239}Pu concentration in VERA 2B assembly at EOC was around thousand times more than that of the VERA 2P assembly which comes from the higher ^{238}U in VERA 2B at first. It can be seen

Table 5. Temperature coefficient of reactivity and effective delayed neutron fraction (β_{eff}).

VERA cases	Burnup condition	Doppler coefficient of reactivity (DTC, $\Delta k/k \text{ K}^{-1}$)	Moderator coefficient of reactivity (MTC, $\Delta k/k \text{ K}^{-1}$)	Effective delayed of neutron fraction (β_{eff})
VERA 2B	BOC	-4.03437E-05	-4.09475E-05	0.00685 ± 0.00010
	MOC	-6.01477E-05	-9.47981E-05	0.00478 ± 0.00008
	EOC	-6.98148E-05	-1.75884E-04	0.00426 ± 0.00008
VERA 2P	BOC	-2.36304E-05	-7.41383E-06	0.00670 ± 0.00009
	MOC	-2.78369E-05	-1.11634E-04	0.00479 ± 0.00008
	EOC	-3.22049E-05	-1.83914E-04	0.00426 ± 0.00008

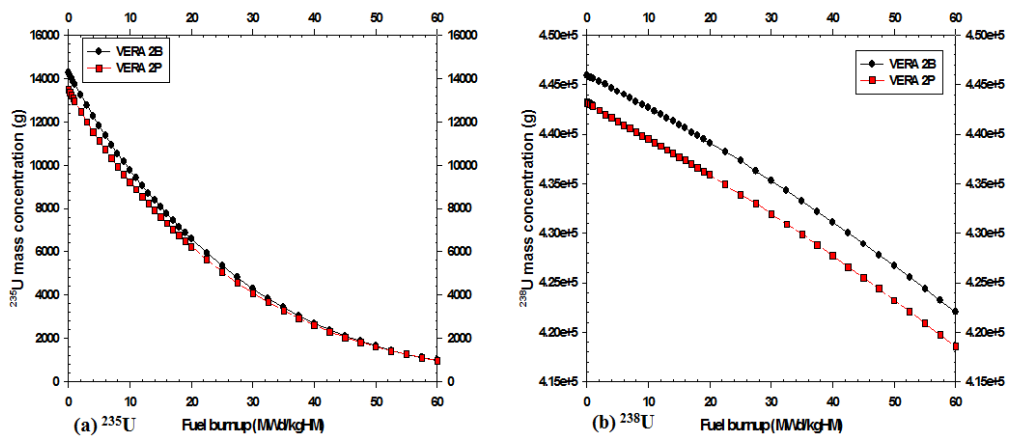


Figure 4. Uranium concentration of benchmark cases.

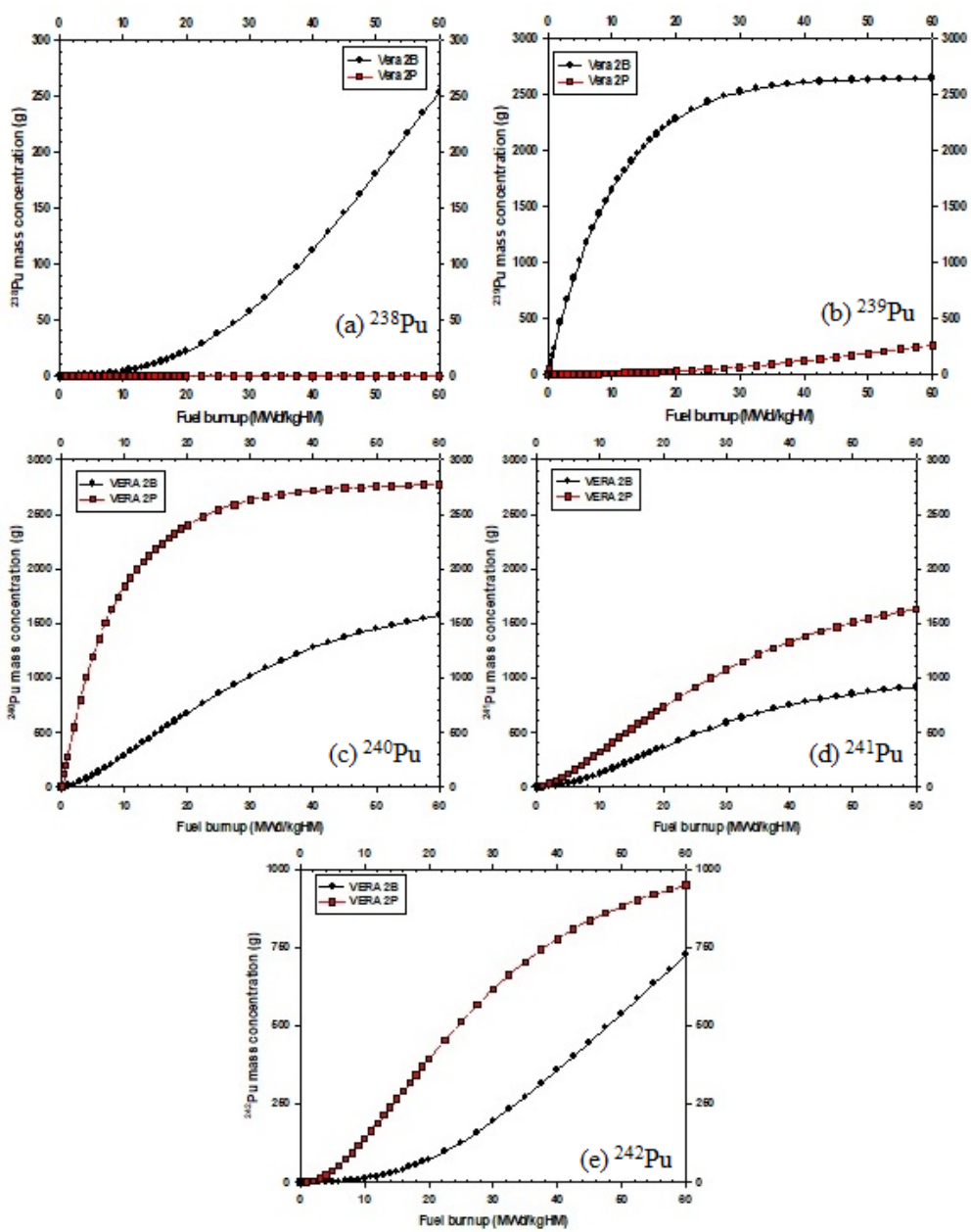


Figure 5. Plutonium concentration of benchmark cases.

in Figure 5(c-e) that the ^{240}Pu , ^{241}Pu , and ^{242}Pu VERA 2P were higher than VERA 2B with similar trends but delayed that might come from the hardened neutron spectrum shifting since thermal neutrons absorbed by gadolinia. ^{241}Pu was a formed when ^{240}Pu captures a neutron while ^{242}Pu was produced by successive neutron capture of ^{239}Pu , ^{240}Pu , and ^{241}Pu . Like some other plutonium isotopes, especially ^{239}Pu , ^{241}Pu was fissile, with a neutron absorption cross section about one-third larger than ^{239}Pu , and a fission probability around 73% similar to the neutron absorption.

4. Conclusion

The MCNP calculation of VERA benchmark cases has been conducted and was in good agreement with the MCS, STREAM, McCARD, and other neutron transport codes. In comparison to the MCS and STREAM, the infinite multiplication factor (k_{inf}) calculated by MCNP shows a good agreement at the BOC with a difference of less than 100 pcm while at MOC and EOC were within the range of 200 – 700 pcm. In comparison to the benchmark data by McCARD, it was found that the results show a good agreement at the BOC, but at MOC-EOC the deviations were within the range of 175 – 1500 pcm which might come from differences in nuclear data being used. The DTC of both cases were negative which was lower than $-4 \times 10^{-5} \Delta k/k \text{ K}^{-1}$ for VERA 2B case and lower than $-2 \times 10^{-5} \Delta k/k \text{ K}^{-1}$ for VERA 2P case. On another hand, the MTC was lower than $-4 \times 10^{-5} \Delta k/k \text{ K}^{-1}$ and $-7 \times 10^{-6} \Delta k/k \text{ K}^{-1}$ for VERA 2B and 2P cases respectively, while both became more negative as fuel burned. The β_{eff} values of VERA 2B and VERA 2P were 685 and 670 pcm respectively, since both use ^{235}U fissile nuclear material, and slightly decrease caused by other fissile material being produced through fuel burnup. The ^{235}U concentration of VERA 2B fuel assembly at BOC was around ~ 600 gr higher than VERA 2P assembly, with almost the same amount on EOC, around ~ 1000 gr since VERA 2P case has lower fissile material content and lower heavy metal loading due to 24 mixed fuel pins. The discrepancy in plutonium concentration between VERA 2B and 2P cases comes from the hardened neutron flux on case 2P caused by mixed uranium-gadolinia fuel pin. It can be concluded that these findings can be used for further calculation on the whole core analysis.

Acknowledgments

We would like to express our sincere gratitude to Dr. Eng. Topan Setiadipura and Dr. Anis Rohanda for their motivations and moral support during the research work. We would also like to express our sincere gratitude to Prof. Dr. Eng. Zaki Su'ud from the Nuclear Physics and Biophysics Research Division, Physics Department, Institut Teknologi Bandung (ITB) for granting us permission to use the MCNP6 code license in our simulations.

Authors Contributions

All the authors have participated equally in the intellectual content, conception and design of this work or the analysis and interpretation of the data, as well as the writing of the manuscript.

Availability of data and materials

Data presented in the manuscript are available via request.

Conflict of Interests

The author declare that they have no known competing financial interests or personal relationships that could have appeared to influence the work reported in this paper.

Open Access

This article is licensed under a Creative Commons Attribution 4.0 International License, which permits use, sharing, adaptation, distribution and reproduction in any medium or format, as long as you give appropriate credit to the original author(s) and the source, provide a link to the Creative Commons license, and indicate if changes were made. The images or other third party material in this article are included in the article's Creative Commons license, unless indicated otherwise in a credit line to the material. If material is not included in the article's Creative Commons license and your intended use is not permitted by statutory regulation or exceeds the permitted use, you will need to obtain permission directly from the OICC Press publisher. To view a copy of this license, visit <https://creativecommons.org/licenses/by/4.0>.

References

- [1] Z. Su'ud and H. Sekimoto. "The prospect of gas cooled fast reactors for long life reactors with natural uranium as fuel cycle input." *Annals of Nuclear Energy*, **54**:58, 2013. DOI: <https://doi.org/10.1016/j.anucene.2012.09.014>.
- [2] H. Yu, J. Cai, S. He, and X. Li. "Analysis of neutron physics and thermal hydraulics for fuel assembly of small modular reactor loaded with ATFs." *Annals of Nuclear Energy*, **152**:107957, 2023. DOI: <https://doi.org/10.1016/j.anucene.2020.107957>.
- [3] J. Vujić, D. P. Antić, and Z. Vukmirović. "Environmental impact and cost analysis of coal versus nuclear power: The U.S. case." *Energy*, **45**:31, 2012. DOI: <https://doi.org/10.1016/j.energy.2012.02.011>.
- [4] S. Hirdaris, Y. Cheng, P. Shallcross, J. Bonafoux, D. Carlson, B. Prince, and G. Sarris. "Considerations on the potential use of nuclear small modular reactor (SMR) technology for merchant marine propulsion." *Ocean Engineering*, **79**:101, 2014. DOI: <https://doi.org/10.1016/j.oceaneng.2013.10.015>.

- [5] S. Hirdaris, Y. Cheng, P. Shallcross, J. Bonafoux, D. Carlson, and G. Sarris. "Concept design for a suezmax tanker powered by a 70 MW small modular reactor.". *Transactions of the Royal Institution of Naval Architects Part A: International Journal of Maritime Engineering*, **156**:37, 2014. DOI: <https://doi.org/10.3940/rina.ijme.2014.al.276>.
- [6] IAEA. "Advances in small modular reactor technology developments - A supplement to: IAEA advanced reactors information system.". *ARIS*, , 2020.
- [7] E. Hussein. "Emerging small modular nuclear power reactors: A critical review.". *Physics Open*, **5**:100038, 2020. DOI: <https://doi.org/10.1016/j.physo.2020.100038>.
- [8] S. K. Kang. "Specification for the VERA Depletion Benchmark Suite.". *Consortium for Advanced Simulation of LWRs*, , 2015. DOI: <https://doi.org/10.2172/1256820>.
- [9] K. S. Kim, D. H. Lee, H. J. Shim, and A. J. Pawel. "VERA depletion benchmarks by CASL VERA, Serpent and McCard with ENDF/B-VII.0 and VII.1.". *PHYSOR: Reactor Physics Paving The Way Towards More Efficient Systems. Cancun, Mexico*, , 2018.
- [10] J. Park, A. Khassenov, W. Kim, S. Choi, and D. Lee. "Comparative analysis of VERA depletion benchmark through consistent code-to-code comparison.". *Annals of Nuclear Energy*, **124**:385, 2019. DOI: <https://doi.org/10.1016/j.anucene.2018.10.024>.
- [11] J. Yu and B. Forget. "Verification of depletion capability of OpenMC using VERA depletion benchmark.". *Annals of Nuclear Energy*, **170**:108973, 2022. DOI: <https://doi.org/10.1016/j.anucene.2022.108973>.
- [12] H. J. Park, D. H. Lee, B. K. Jeon, and H. J. Shim. "Monte Carlo burnup and its uncertainty propagation analyses for VERA depletion benchmarks by McCARD.". *Nuclear Engineering and Technology*, **50**:1043, 2018. DOI: <https://doi.org/10.1016/j.net.2018.06.003>.
- [13] A. O. Albugami, A. S. Alomari, and A. I. Almarshad. "Modeling and simulation of VERA core physics benchmark using OpenMC code.". *Nuclear Engineering and Technology*, **55**:3388–3400, 2023. DOI: <https://doi.org/10.1016/j.net.2023.05.036>.
- [14] B. Collins, A. Godfrey, S. Stimpson, and S. Palmtag. "Simulation of the BEAVRS benchmark using VERA.". *Annals of Nuclear Energy*, **145**:107602, 2020. DOI: <https://doi.org/10.1016/j.anucene.2020.107602>.
- [15] T. D. C. Nguyen, H. Lee, S. Choi, and D. Le. "Validation of UNIST Monte Carlo code MCS using VERA progression problems.". *Nuclear Engineering and Technology*, **52**:878, 2020. DOI: <https://doi.org/10.1016/j.net.2019.10.023>.
- [16] N. N. T. Mai, K. Kim, M. Lemaire, T. D. C. Nguyen, W. Lee, and D. Lee. "Analysis of several VERA benchmark problems with the photon transport capability of STREAM.". *Nuclear Engineering and Technology*, **54**:2670, 2022. DOI: <https://doi.org/10.1016/j.net.2022.02.004>.
- [17] J. T. Goorley, M. R. James, T. E. Booth, F. B. Brown, J. S. Bull, L. J. Cox, J. W. Durkee Jr, J. S. Elson, M. L. Fensin, R. A. Forster, et al. "Initial MCNP6 Release Overview - MCNP6 Version 1.0.". *LANL Report LA-UR-13-22934. Affiliation: Los Alamos National Laboratory*, , 2013. DOI: <https://doi.org/10.2172/1086758>.
- [18] M. B. Chadwick, M. Herman, P. Obložinský, M. E. Dunn, Y. Danon, A. C. Kahler, D. L. Smith, B. Pritychenko, G. Arbanas, R. Arcilla, et al. "ENDF/B-VII.1 nuclear data for science and technology: cross sections, covariances, fission product yields and decay data.". *Nuclear Data Sheets*, **112**:2887, 2011. DOI: <https://doi.org/10.1016/j.nds.2011.11.002>.
- [19] C. M. Read Jr, T. W. Knight, and K. S. Allen. "Using a modified CINDER90 routine in MCNPX 2.6.0 for the prediction of helium production in minor actinide targets.". *Nuclear Engineering and Design*, **241**:5033, 2011. DOI: <https://doi.org/10.1016/j.nucengdes.2011.09.016>.
- [20] Z. Zuhair, W. Luthfi, S. Sriyono, S. Suwoto, and T. Setiadi-pura. "Study on kinetic parameters characteristics of pebble bed reactor using HTR-Proteus.". *Nuclear Technology & Radiation Protection*, **38**:1–19, 2023. DOI: <https://doi.org/10.2298/NTRP2202119Z>.
- [21] Zuhair, R. A. P. Dwijayanto, Sriyonoa, Suwoto, and Z. Su'ud. "Preliminary Study on TRU Transmutation in VVER-1000 Fuel Assembly using MCNP.". *Kerntechnik*, **87**:305, 2022. DOI: <https://doi.org/10.1515/kern-2021-1017>.
- [22] O. Kabach, A. Chetaine, A. Benchrifia, H. Amsil, and F. El Banni. "A comparative analysis of the neutronic performance of thorium mixed with uranium or plutonium in a high temperature pebble-bed reactor.". *International Journal of Energy Research*, **45**:1–18, 2021. DOI: <https://doi.org/10.1002/er.6935>.
- [23] M. Hassan. "Simulation of a full PWR core with MCNP.". *International Journal of Science and Research*, **9**:913, 2020. DOI: <https://doi.org/10.21275/SR20916224433>.
- [24] Zuhair, R. A. P. Dwijayanto, Suwoto, and T. Setiadi-pura. "The implication of thorium fraction on neutronic parameters of pebble bed reactor.". *Kuwait Journal of Science*, **48**:1, 2021. DOI: <https://doi.org/10.48129/kjs.v48i3.9984>.
- [25] Zuhair, Suwoto, S. Permana, and T. Setiadi-pura. "Study on control rod reactivity of small pebble bed reactor with wallpaper fuel design.". *Journal Physics: Conference Series*, **1772**:012021, 2021. DOI: <https://doi.org/10.1088/1742-6596/1772/1/012021>.

- [26] Zuhair, Suwoto, T. Setiadipura, and Z. Su'ud. "Study on MCNP6 model in the calculation of kinetic parameters for pebble bed reactor." *Acta Polytechnica*, **60**:175, 2020. DOI: <https://doi.org/10.14311/AP.2020.60.0175>.
- [27] Zuhair, Suwoto, T. Setiadipura, and J. C. Kuijper. "The effects of fuel type on control rod reactivity of pebble-bed reactor." *Nukleonika*, **64**:131, 2019. DOI: <https://doi.org/10.1088/1742-6596/1772/1/012021>.
- [28] Kabach, A. Chetaine, A. Benchrif, and H. Amzil. "The use of burnable absorbers integrated into TRISO/QUADRISO particles as a reactivity control method in a pebble-bed HTR reactor fuelled with (Th, ²³³U)O₂." *Nuclear Engineering and Design*, **384**:111476, 2021. DOI: <https://doi.org/10.1016/j.nucengdes.2021.111476>.
- [29] M. A. Alzamly, M. Aziz, A. A. Badawi, H. Abou-Gabal, and A. R. A. Gadallah. "Burnup analysis for HTR-10 reactor core loaded with uranium and thorium oxide." *Nuclear Engineering and Technology*, **52**:674, 2020. DOI: <https://doi.org/10.1016/j.net.2019.09.012>.
- [30] Zuhair, Suwoto, T. Setiadipura, and J. C. Kuijper. "Study on the characteristics of effective delayed neutron fraction (β_{eff}) for pebble bed reactor with plutonium fuel." *Iranian Journal of Science and Technology, Transaction A: Science*, **43**:3037, 2019. DOI: <https://doi.org/10.1007/s40995-019-00772-8>.
- [31] Zuhair, Suwoto, T. Setiadipura, and Z. Su'ud. "The effects of applying silicon carbide coating on core reactivity of pebble-bed HTR in water ingress accident." *Kerntechnik*, **82**:92, 2017. DOI: <https://doi.org/10.3139/124.110628>, 2017.
- [32] J. P. Carter and R. A. Borrelli. "Integral molten salt reactor neutron physics study using Monte Carlo N-particle code." *Nuclear Engineering and Design*, **65**:110718, 2020. DOI: <https://doi.org/10.1016/j.nucengdes.2020.110718>.
- [33] A. Facchini, V. Giusti, R. Ciolini, K. Tuček, D. Thomas, and E. D'Agata. "Detailed neutronic study of the power evolution for the European sodium fast reactor during a positive insertion of reactivity." *Nuclear Engineering and Design*, **313**:1, 2017. DOI: <https://doi.org/10.1016/j.nucengdes.2016.11.014>.
- [34] Zuhair, R. A. P. Dwijayanto, H. Adrial, Suwoto, and T. Setiadipura. "Neutronic effect of utilizing TRISO particles on core characteristics of experimental power reactor." *AIP Conference Proceedings*, **2180**:020005, 2019. DOI: <https://doi.org/10.1063/1.5135514>.
- [35] Zuhair, Suwoto, H. Adrial, and T. Setiadipura. "Study on MOX core characteristics of experimental power reactor using MCNP6 code." *Journal Physics: Conference Series*, **1198**:022031, 2019. DOI: <https://doi.org/10.1088/1742-6596/1198/2/022031>.
- [36] P. H. Liem, Zuhair, and D. Hartanto. "Sensitivity and uncertainty analysis on the first core criticality of the RSG GAS multipurpose research reactor." *Progress in Nuclear Energy*, **114**:46, 2019. DOI: <https://doi.org/10.1016/j.pnucene.2019.03.001>.
- [37] Suwoto and Zuhair. "Analisis sensitivitas ketebalan reflektor grafit teras RGTT200K menggunakan perhitungan Monte Carlo." *Jurnal Pengembangan Energi Nuklir*, **16**:73, 2014.
- [38] J. J. Lee, C. Kong, and D. Lee. "Status of Monte Carlo code development at UNIST." *Proceedings of the PHYSOR Conference, Kyoto, Japan Atomic Energy Agency*, , 2014. DOI: <https://doi.org/10.11484/jaea-conf-2014-003>.
- [39] S. Choi, W. Kim, J. Choe, W. Lee, H. Kim, B. Ebiwonjumi, E. Jeong, K. Kim, D. Yun, H. Lee, and D. Lee. "Development of high-fidelity neutron transport code STREAM." *Computer Physics Communications*, **264**:107915, 2021. DOI: <https://doi.org/10.1016/j.cpc.2021.107915>.